Supporting Information

Introducing π-electron-rich aromatic rings into a robust Zr-MOF for efficient natural gas purification and C_3H_8/*n*-C_4H_{10} recovery

Liu-Li Meng, Xiao-Hong Xiong, Liang Zhang, Liang Song, Cheng-Xia Chen*, Zhang-Wen Wei*, Cheng-Yong Su*

MOE Laboratory of Bioinorganic and Synthetic Chemistry, GBRCE for Functional Molecular Engineering, Lehn Institute of Functional Materials, IGCME, School of Chemistry, Sun Yat-Sen University, Guangzhou 510275, China.

Zr-MOF; Breakthrough; nature gas; gas separation; n-C_4H_{10} recovery.

E-mail: weizhw3@mail.sysu.edu.cn;
chenchx29@mail.sysu.edu.cn;
cesscy@mail.sysu.edu.cn

Table of Contents

S1. Materials and Instrumentation

General procedures. All the reagents and solvents were commercially available and directly utilized without further purification. Powder X-ray diffraction (PXRD) was carried out with a Rigaku SmartLab diffractometer (Bragg-Brentano geometry, Cu $K_{\alpha 1}$ radiation, λ = 1.54178 Å). Solid-state IR spectra were recorded using Nicolet/Nexus-670 FT-IR spectrometer in the region of 4000-400 cm^{-1} using KBr pellets. Thermogravimetric analyses (TGA) were performed on a NETZSCH TG209 system in nitrogen and under 1 atm of pressure at a heating rate of 5 °C min^{-1}. 77 K N_2 sorption measurements were conducted using QUADRASORB EVO gas adsorption analyzer. Gas adsorption isotherms for pressures in the range of 0-1.0 bar were obtained by a volumetric method using a Quantachrome autosorb-iQ_2-MP gas adsorption analyzer. Breakthrough experiments were collected by two different instruments, BSD-MAB (Multi-component Adsorption Breakthrough Curve Analyzer) with mass spectrometer as detector, and a self-built instrument with gas chromatography (FL-9790 plus) as detector.

Synthesis of 6-(4-carboxyphenyl)-2-naphthalenecarboxylic acid (H_2L).[1] To a solution of methyl 6-bromo-2-napthoate (2.65 g, 10 mmol) in 125 mL of toluene was added the mixture of (4-(methoxycarbonyl)phenyl)boronic acid (2.34 g, 13 mmol) in 30 mL of ethanol, followed by the addition of a solution of Na_2CO_3 (3.5 g, 33 mmol) in 10 mL water. This solution was degassed using N_2 for 10 min, and then $Pd(PPh_3)_4$ (0.5 g, 0.43 mmol) was added. The resulting reaction mixture was stirred at 90 °C under N_2 overnight. The solvent was then removed using rotary evaporation, and the residue was dissolved in CH_2Cl_2 and washed with water. The organic layer was next dried over $MgSO_4$, filtered, concentrated, and purified by silica gel flash column chromatography with an eluent of dichloromethane: petroleum ether = 1:8 (v/v). The product was hydrolyzed by refluxing in 2 M NaOH solution (ethanol : water = 1 : 1) for 48 h followed by acidification with pH = 1 aqueous HCl to afford H_2L as white solid. Yield = 2.4 g (82.2%). ^{1}H NMR (DMSO-d_6, δ ppm): 13.08 (s, 2H, COOH), 8.65 (s, 1H, ArH), 8.40 (s, 1H, ArH), 8.24 (d, 1H, ArH), 8.13-8.06 (m, 3H, ArH), 8.04-7.97 (d, 4H, ArH).

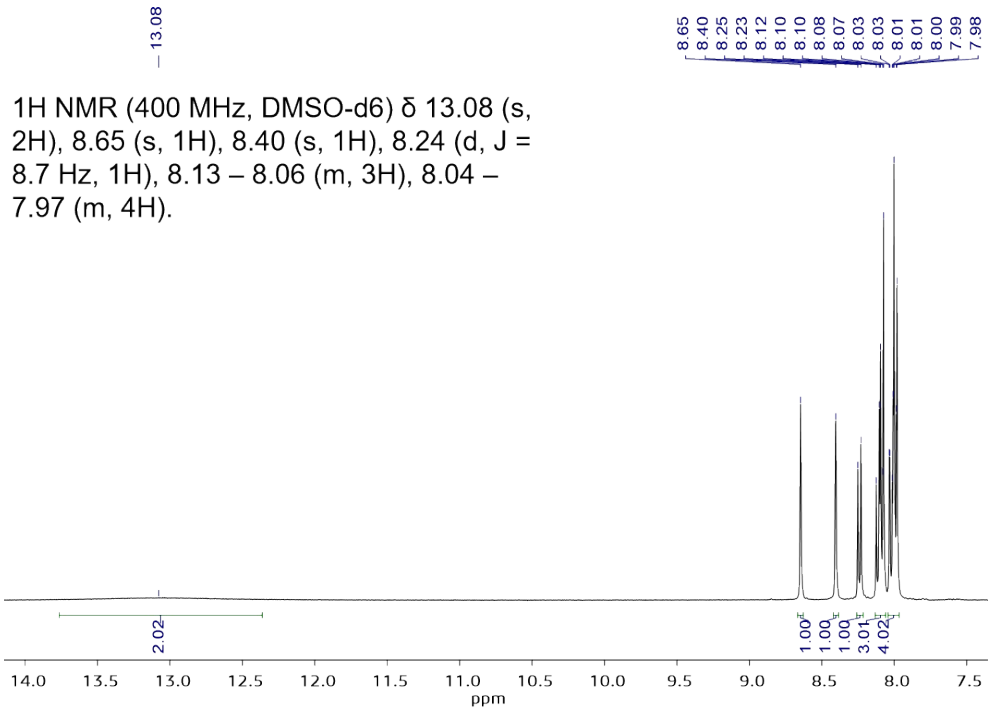

Figure S1. ^{1}H NMR spectrum of H_2L.

Synthesis of $[Zr_6(\mu_3\text{-}OH)_4(\mu_3\text{-}O)_4(L)_6]\cdot$xGuest (LIFM-233). $ZrCl_4$ (20.0 mg, 0.086 mmol) and H_2L (25.1 mg, 0.086 mmol) were mixed with 0.2 mL of trifluoroacetic acid (TFA) in 5 mL of *N,N*-dimethylformamide (DMF). To this was added with stirring. The mixture was sealed in a Pyrex tube and heated to 120 °C or 72 h. The colorless block crystals obtained were filtered and washed with DMF. Yield (based on metal source) = 73.6%.

Sample activation. The as-synthesized sample of LIFM-233 was soaked in acetone for 3 days with acetone refreshing every 8 hours. Then, the acetone-exchanged sample was activated at 80 °C under vacuum for 10 hours to give the activated LIFM-233.

S2. Single Crystal X-Ray Crystallography

The single-crystal of LIFM-233 was picked and coated in para tone oil, attached to a glass silk which was inserted in a stainless stick, then transferred to the Rigaku SmartLab diffractometer with the Enhance X-ray Source of Cu radiation (λ = 1.54178 Å) using the ω-ϕ scan technique. The structure was solved by direct methods and refined by full-matrix least squares against F^2 using the SHELXL programs.[2] Hydrogen

atoms were placed in geometrically calculated positions and included in the refinement process using riding model with isotropic thermal parameters: Uiso (H) = 1.2 Ueq (-CH). All the electrons of disordered solvent molecules which cannot be determined, are removed by SQUEEZE routine of PLATON program.[3] Crystal data and refinement parameters are listed in Table S1.

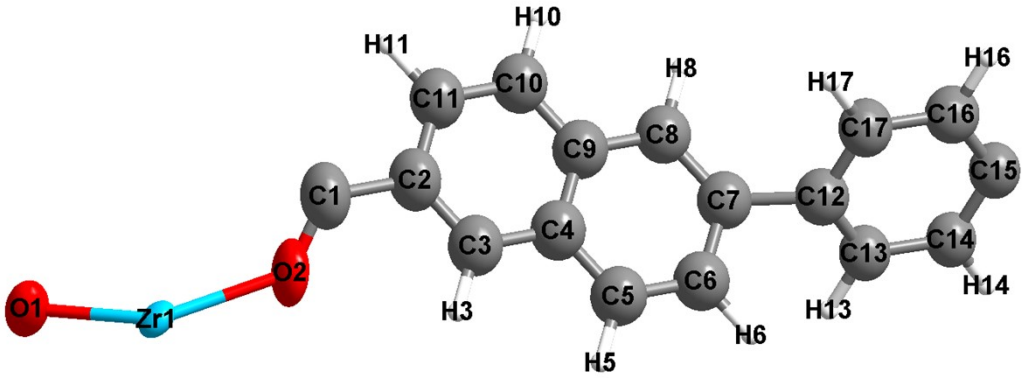

Figure S2. The asymmetric unit of LIFM-233.

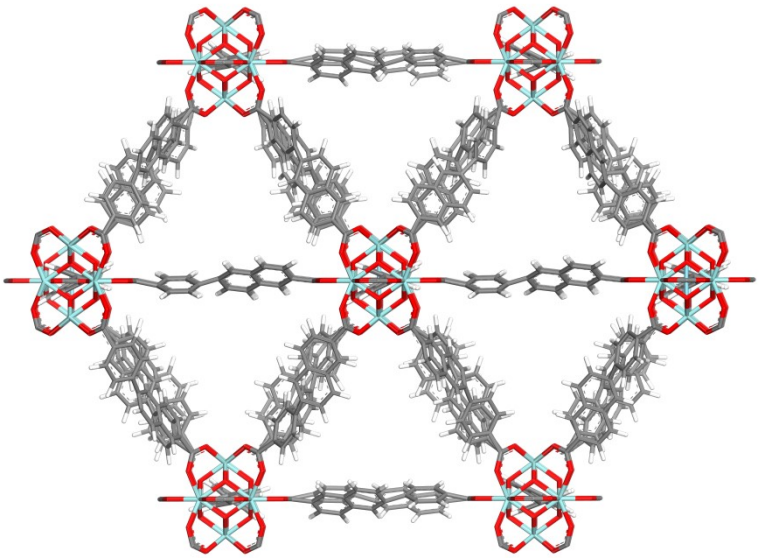

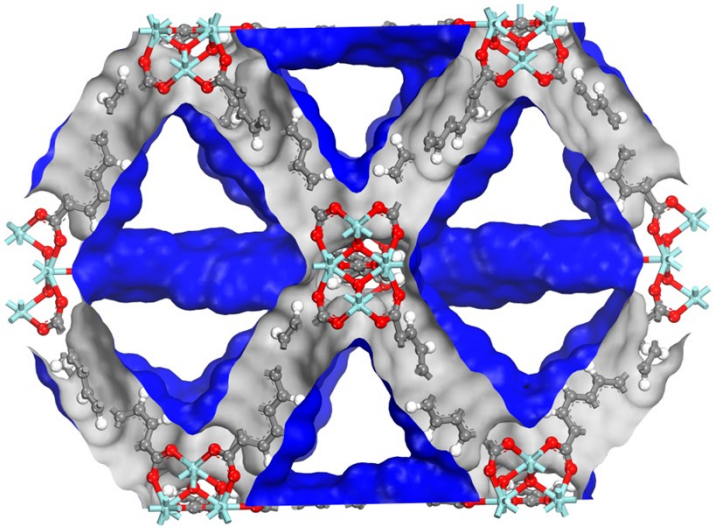

Figure S3. The structure and corresponding solvent accessible surface in LIFM-233. Structural disorder has been removed for clarity.

S3. PXRD, TG and IR Analysis

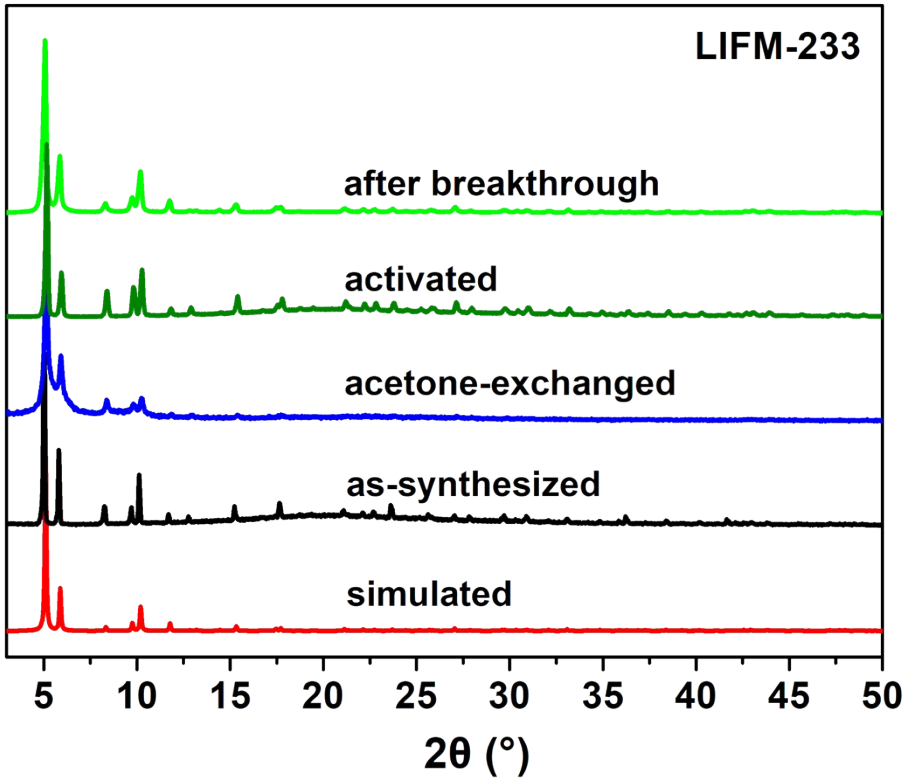

Figure S4. The PXRD patterns of LIFM-233.

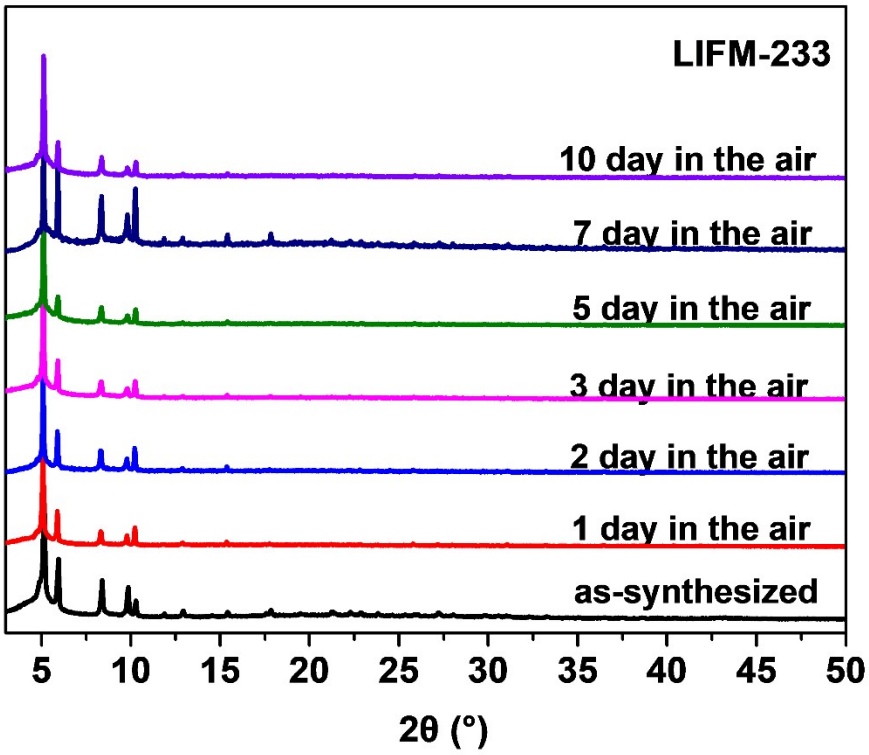

Figure S5. The stability tests of LIFM-233 in the air.

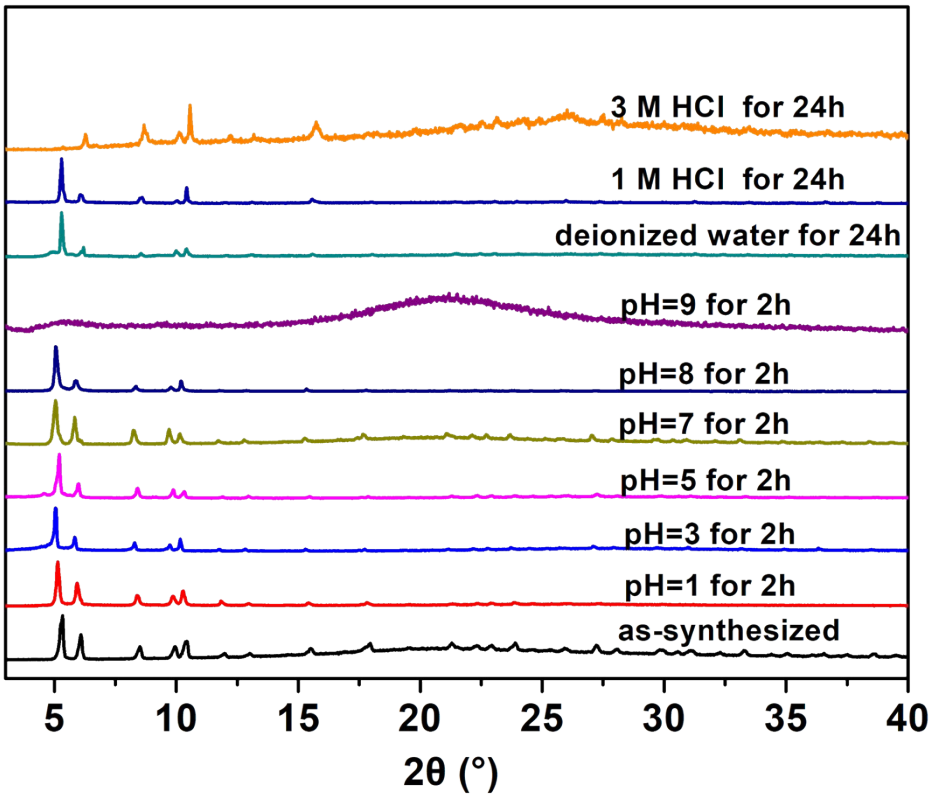

Figure S6. The PXRD patterns of LIFM-233 after immersing the samples into aqueous solutions with different pH values.

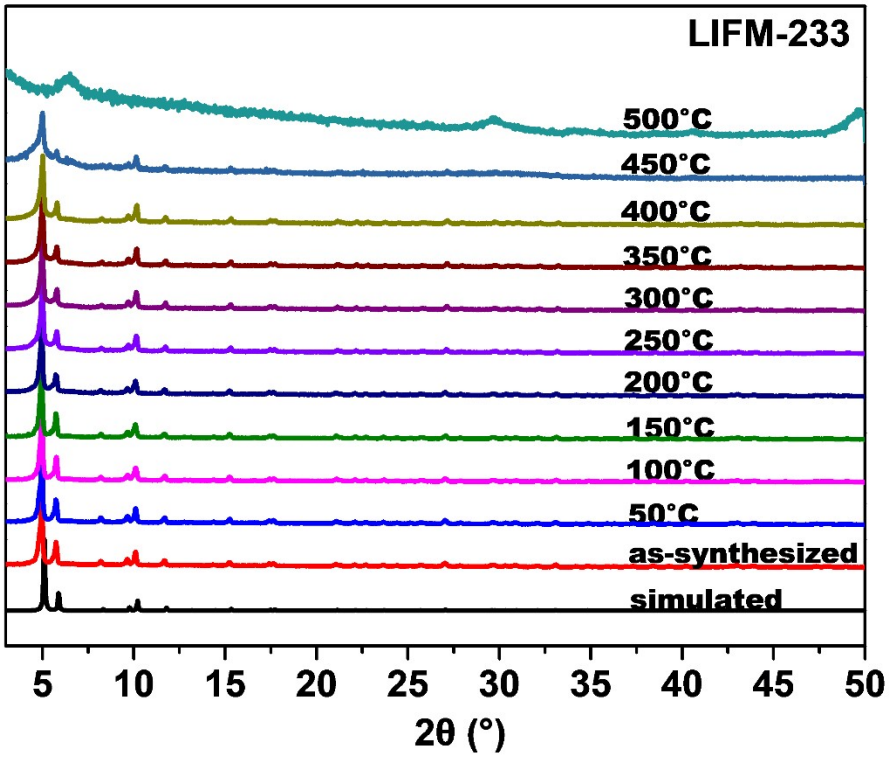

Figure S7. The variable-temperature PXRD patterns of LIFM-233.

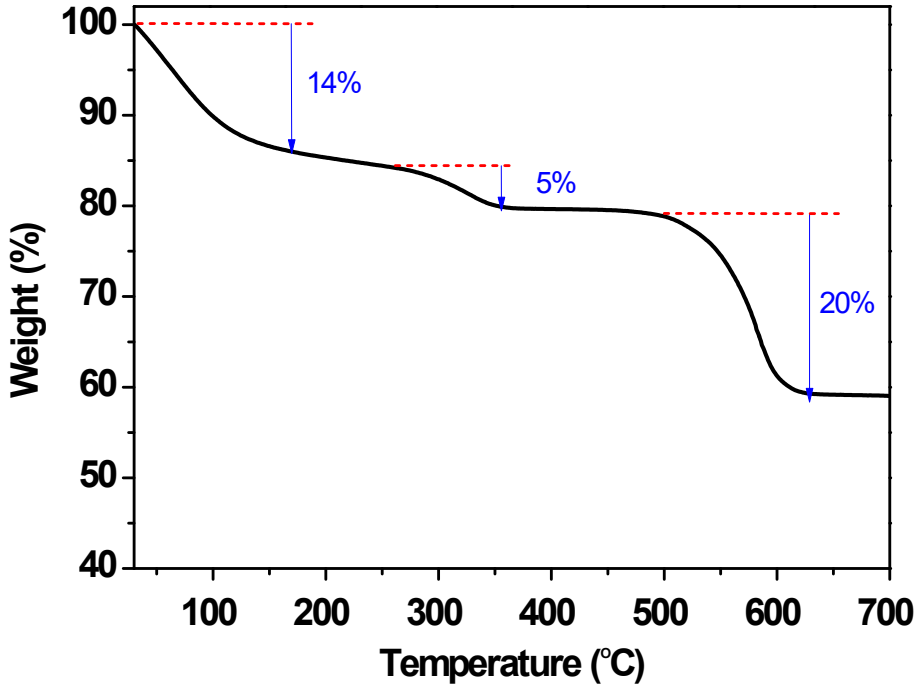

Figure S8. The thermogravimetric analysis (TGA) of LIFM-233.

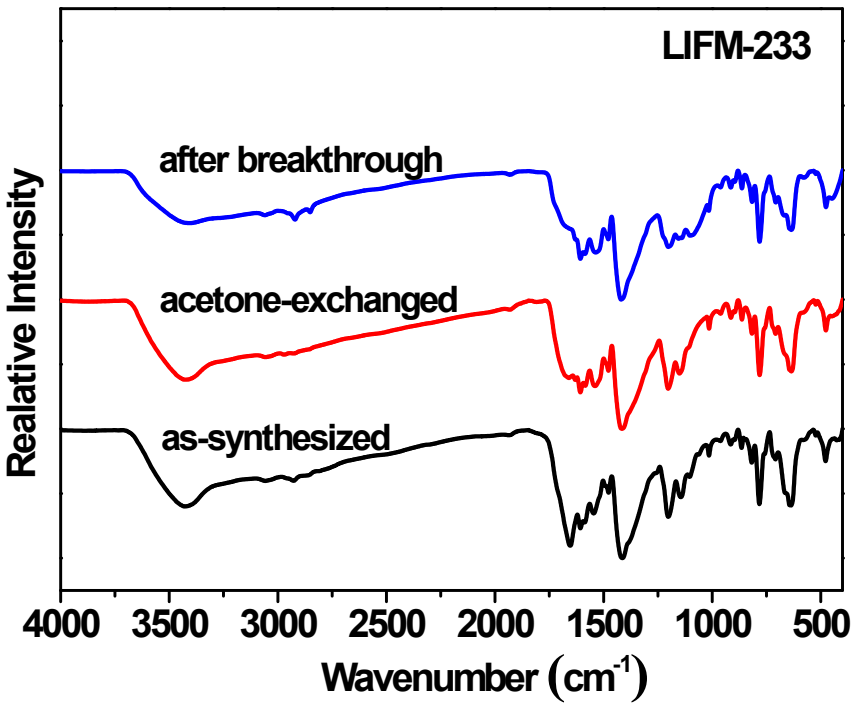

Figure S9. The infrared spectra of LIFM-233.

S4. Gas Sorption Measurements

Gas Sorption Isotherms: The N_2 gas sorption isotherm of activated LIFM-233 was performed on a QUADRASORB EVO gas adsorption analyzer. Low pressure sorption isotherms of CH_4, C_2H_6, C_3H_8 and n-C_4H_{10} gases were performed on a Quantachrome autosorb-iQ2-MP gas adsorption analyzer. For all isotherms, ultra-high purity He gas was used for the estimation of the free space (warm and cold), assuming that it is not adsorbed at any of the studied temperatures. Their corresponding calculation fittings are plotted.

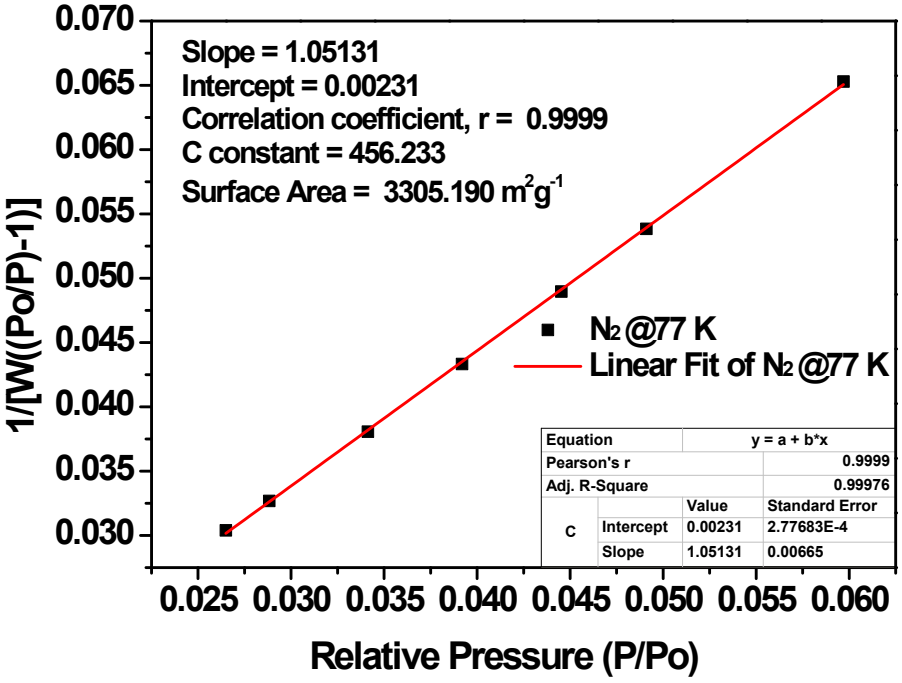

Figure S10. Plot of the linear region for BET equation of activated LIFM-233.

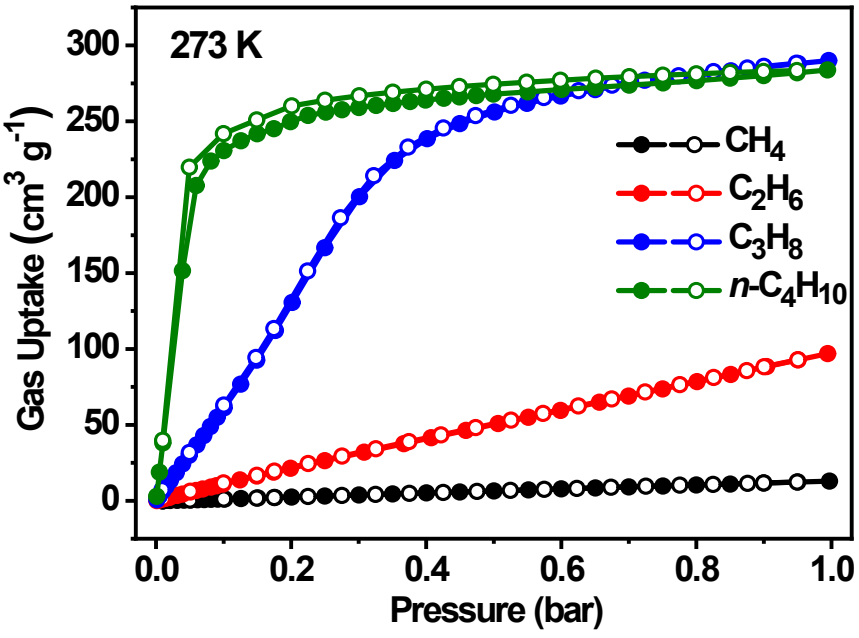

Figure S11. CH_4, C_2H_6, C_3H_8 and n-C_4H_{10} sorption isotherms at 273 K for activated LIFM-233.

S5. Isosteric Heats of Gas Adsorption

A virial-type[4] expression comprising the temperature-independent parameters a_i and b_j was employed to calculate the enthalpies of adsorption for CH_4, C_2H_6, C_3H_8 and n-C_4H_{10} (at 273 and 298 K) on activated LIFM-233. In each case, the data were fitted using the equation:

$$\ln P = \ln N + 1/T \sum_{i=0}^{m} a_i N^i + \sum_{j=0}^{n} b_j N^j \qquad (1)$$

Here, P is the pressure expressed in Torr, N is the amount adsorbed in mmol/g, T is thetemperature in K, a_i and b_j are virial coefficients, and m, n represent the number of coefficients required to adequately describe the isotherms (m and n were gradually increased until the contribution of extra added a and b coefficients was deemed to be statistically insignificant towards the overall fit, and the average value of the squared deviations from the experimental values was minimized). The values of the virial coefficients a_0 through a_m were then used to calculate the isosteric heat of adsorption using the following expression.

$$Q_{st} = -R \sum_{i=0}^{m} a_i N^i \qquad (2)$$

Q_{st} is the coverage-dependent isosteric heat of adsorption and R is the universal gas constant. The heat of CH_4, C_2H_6, C_3H_8 and n-C_4H_{10} sorption for activated LIFM-233 in the manuscript are determined by using the sorption data measured in the pressure range from 0-1 bar (273 K and 298 K), which is fitted by the virial-equation well.

(a)

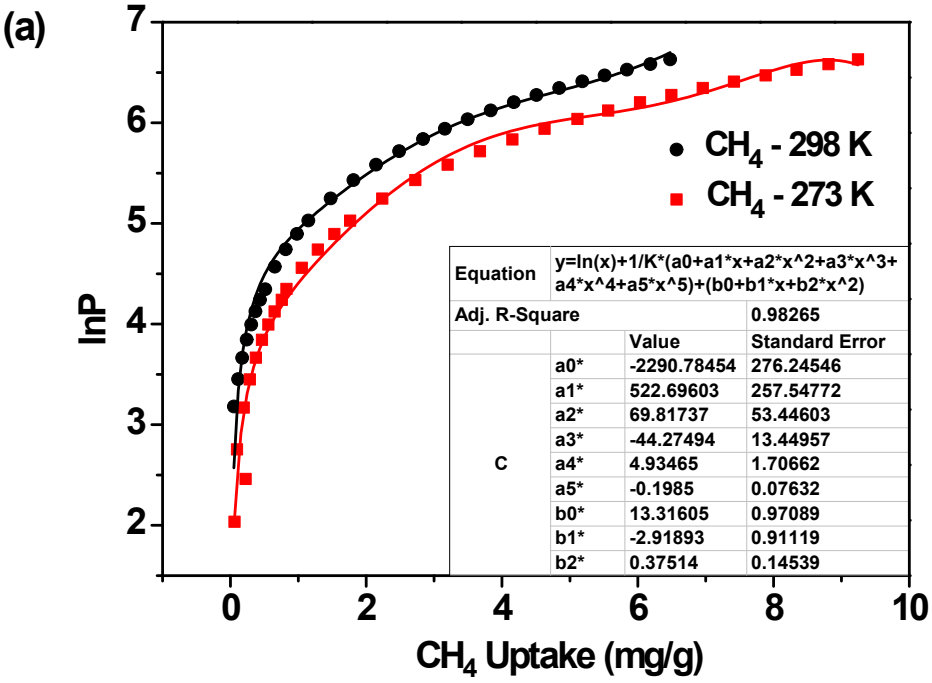

Equation	y=ln(x)+1/K*(a0+a1*x+a2*x^2+a3*x^3+a4*x^4+a5*x^5)+(b0+b1*x+b2*x^2)		
Adj. R-Square			0.98265
		Value	Standard Error
C	a0*	-2290.78454	276.24546
	a1*	522.69603	257.54772
	a2*	69.81737	53.44603
	a3*	-44.27494	13.44957
	a4*	4.93465	1.70662
	a5*	-0.1985	0.07632
	b0*	13.31605	0.97089
	b1*	-2.91893	0.91119
	b2*	0.37514	0.14539

(b)

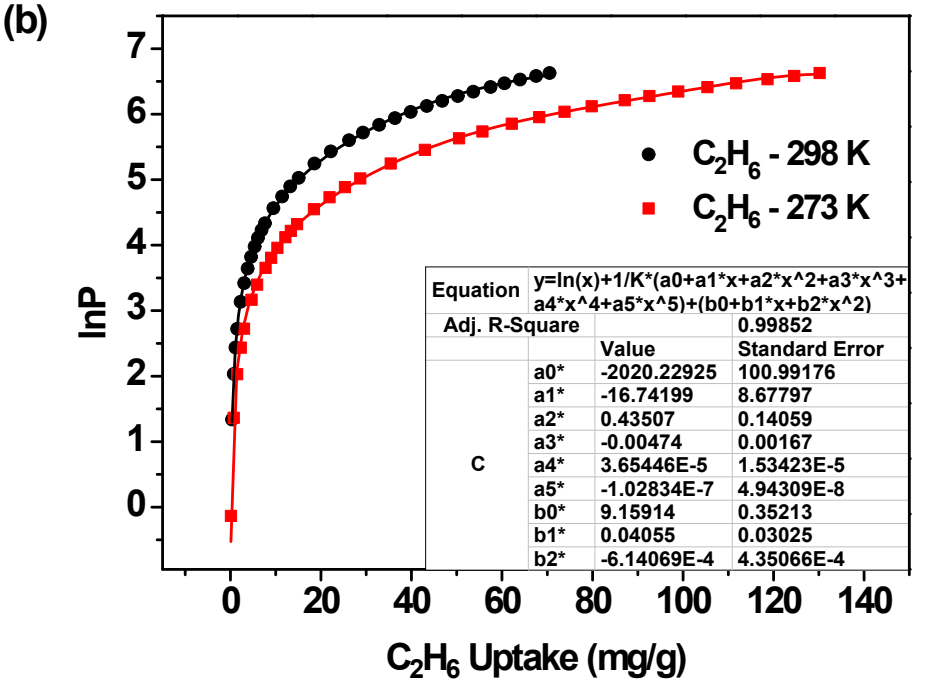

Equation	y=ln(x)+1/K*(a0+a1*x+a2*x^2+a3*x^3+a4*x^4+a5*x^5)+(b0+b1*x+b2*x^2)		
Adj. R-Square			0.99852
		Value	Standard Error
C	a0*	-2020.22925	100.99176
	a1*	-16.74199	8.67797
	a2*	0.43507	0.14059
	a3*	-0.00474	0.00167
	a4*	3.65446E-5	1.53423E-5
	a5*	-1.02834E-7	4.94309E-8
	b0*	9.15914	0.35213
	b1*	0.04055	0.03025
	b2*	-6.14069E-4	4.35066E-4

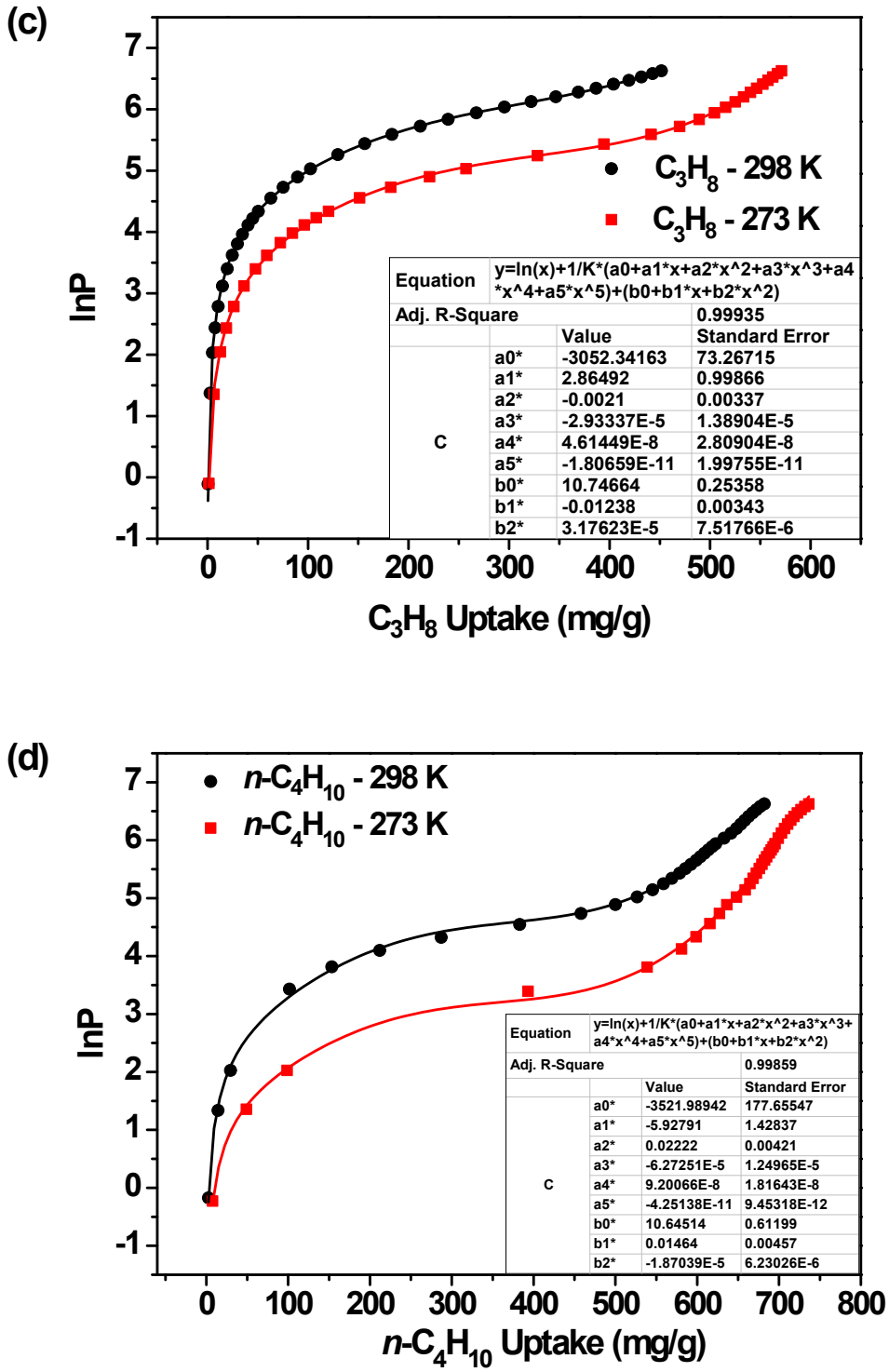

Figure S12. (a) CH_4, (b) C_2H_6, (c) C_3H_8 and (d) n-C_4H_{10} virial fitting (lines) of the adsorption isotherms of activated LIFM-233 measured at 273 K and 298 K.

S6. IAST Selectivity

IAST (ideal adsorption solution theory)[5, 6] was used to predict binary mixture adsorption from the experimental pure-gas isotherms. In order to perform the integrations required by IAST, the single-component isotherms should be fitted by a proper model. In practice, several methods to do this are available. We found for this set of data that the single-site Langmuir-Freundlich equation (SSLF) was successful in fitting the data. As can be seen in Figure S12, the model fits the isotherms very well.

$$q = \frac{q_{m,1} b_1 p^{1/n}}{1 + b_1 p^{1/n}} \qquad (3)$$

Here, P is the pressure of the bulk gas at equilibrium with the adsorbed phase (kPa), q is the adsorbed amount per mass of adsorbent (mmol/g), $q_{m,1}$ is the saturation capacities of sites (mmol/g), b_1 is the affinity coefficients of sites (1/kPa), and n represents the deviations from an ideal homogeneous surface. The fitted parameters were then used to predict multi-component adsorption with IAST.

The selectivity $S_{A/B}$ in a binary mixture of components A and B is defined as $(x_A/y_A)/(x_B/y_B)$, where x_i and y_i are the mole fractions of component i (i = A, B) in the adsorbed and bulk phases, respectively.

(a)

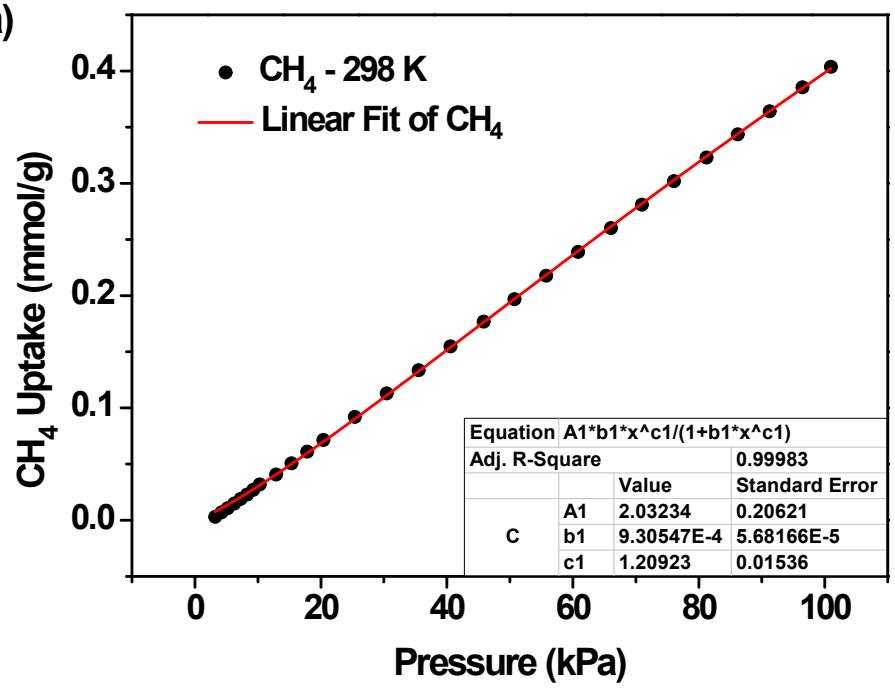

Equation	A1*b1*x^c1/(1+b1*x^c1)		
Adj. R-Square			0.99983
		Value	Standard Error
C	A1	2.03234	0.20621
	b1	9.30547E-4	5.68166E-5
	c1	1.20923	0.01536

(b)

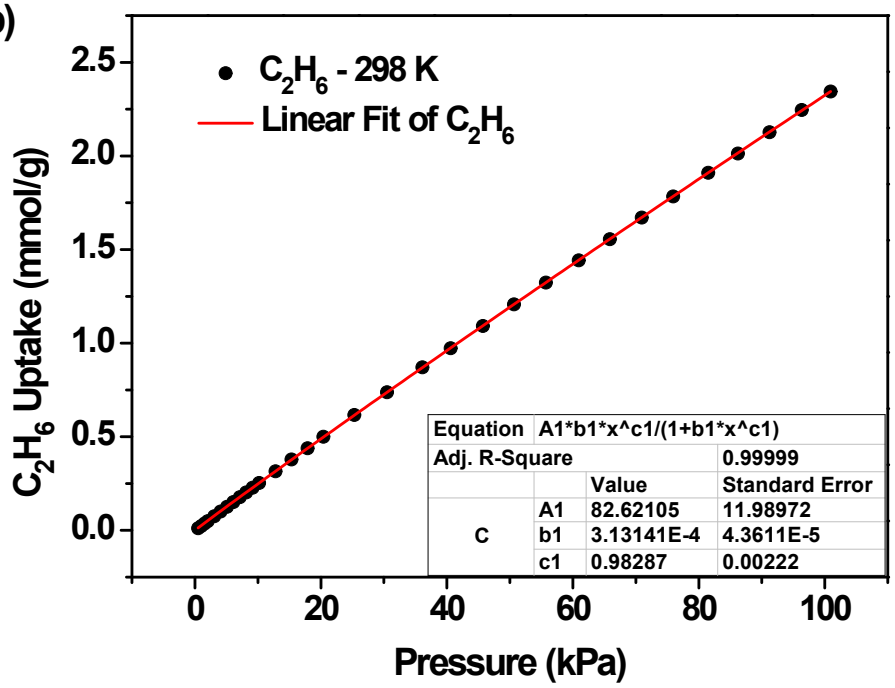

Equation	A1*b1*x^c1/(1+b1*x^c1)		
Adj. R-Square			0.99999
		Value	Standard Error
C	A1	82.62105	11.98972
	b1	3.13141E-4	4.3611E-5
	c1	0.98287	0.00222

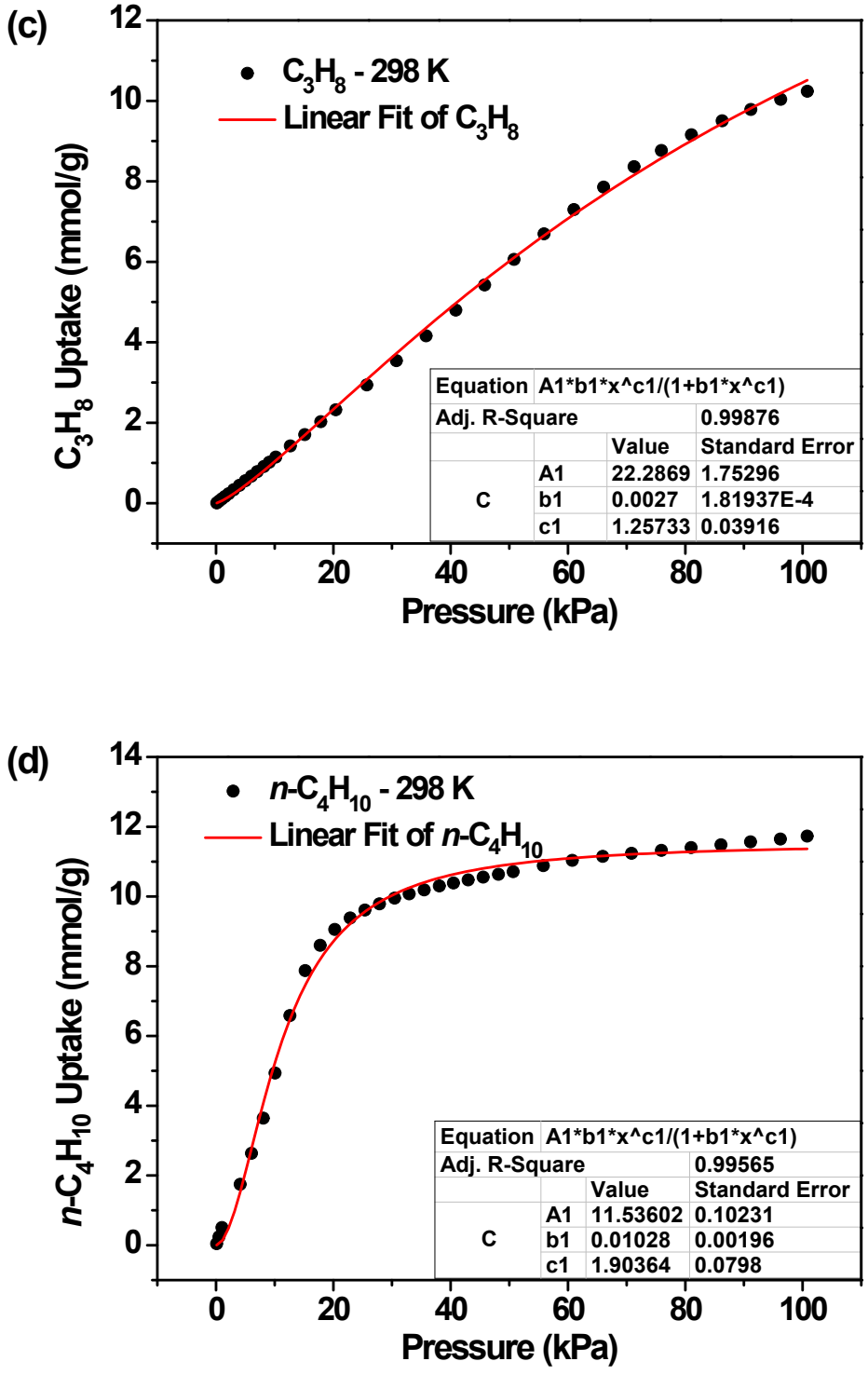

Figure S13. Gas adsorption isotherms and the single-site Langmuir-Freundlich fit lines of CH_4, C_2H_6, C_3H_8 and *n*-C_4H_{10} in activated LIFM-233 at 298 K

S7. Breakthrough Experiments and Recovery

Transient breakthrough experiments for the separation of $CH_4/C_2H_6/C_3H_8$ (85:10:5, v/v/v) were carried out in a fixed bed. The gas flow rates were regulated by mass flow controllers. The column (6 mm inner diameter × 150 mm) contained 0.8 g of pre-activated sample. Before filled in the column, the sample was activated at 333 K for 10 h under vacuum. After sample filling, the column was purged with an He flow (20 mL/min) for 2 h. Then the $CH_4/C_2H_6/C_3H_8$ gas mixture with 3 mL min^{-1} was introduced to the column. The outlet composition was continuously monitored by FULI GC9790 Plus gas chromatograph until a complete breakthrough was achieved. The sample was regenerated with an He flow (20 mL/min) at 333 K for 2 h until all gas signals disappeared before each cyclic experiment.

Transient breakthrough experiments for the separation of $CH_4/C_2H_6/N_2/C_3H_8/n$-C_4H_{10} (85:9:2:3:1, v/v/v/v/v) were carried out in a fixed bed. The column (6 mm inner diameter × 150 mm) contained 0.5 g activated sample (the same batch sample for ternary gas saparation). Before filled in the column, the sample was activated at 333 K for 10 h under vacuum conditions. After sample filling, the column was purged with an He flow (30 mL min^{-1}) for 2 h. Then the $CH_4/C_2H_6/N_2/C_3H_8/n$-C_4H_{10} gas mixture with 10 mL min^{-1} was introduced to the column. The outlet composition was continuously monitored by the mass spectrometer of BSD-MAB multi-constituent adsorption breakthrough curve analyzer until a complete breakthrough was achieved. The sample was regenerated with an He flow (30 mL/min) at 333 K for 2 h until all gas signals disappeared before each cyclic experiment.

Recovery of C_3H_8 and n-C_4H_{10} were carried out. An He stream was flowed over the packed column with flow rate of 20 or 30 mL min^{-1} at 60 ^oC, in which the eluted gas was monitored by a gas chromatograph (for ternary mixture) or a mass spectrometer (for five-component mixture). The purity of the recovered C_3H_8 and n-C_4H_{10} is calculated based on the following equation.

$$\text{Purity}(C_3H_8) = \frac{S_{C_3H_8}}{S_{C_3H_8} + S_{C_2H_6} + S_{CH_4}} \times 100\% \qquad (4)$$

$$\text{Purity}(n\text{-}C_4H_{10}) = \frac{S_{C_3H_8}}{S_{n\text{-}C_4H_{10}} + S_{C_3H_8} + S_{C_2H_6} + S_{CH_4}} \times 100\% \qquad (5)$$

Where S is the integral area of the region bounded by the desorption curve of CH_4, C_2H_6, C_3H_8 or *n*-C_4H_{10} with the X-axis, respectively.

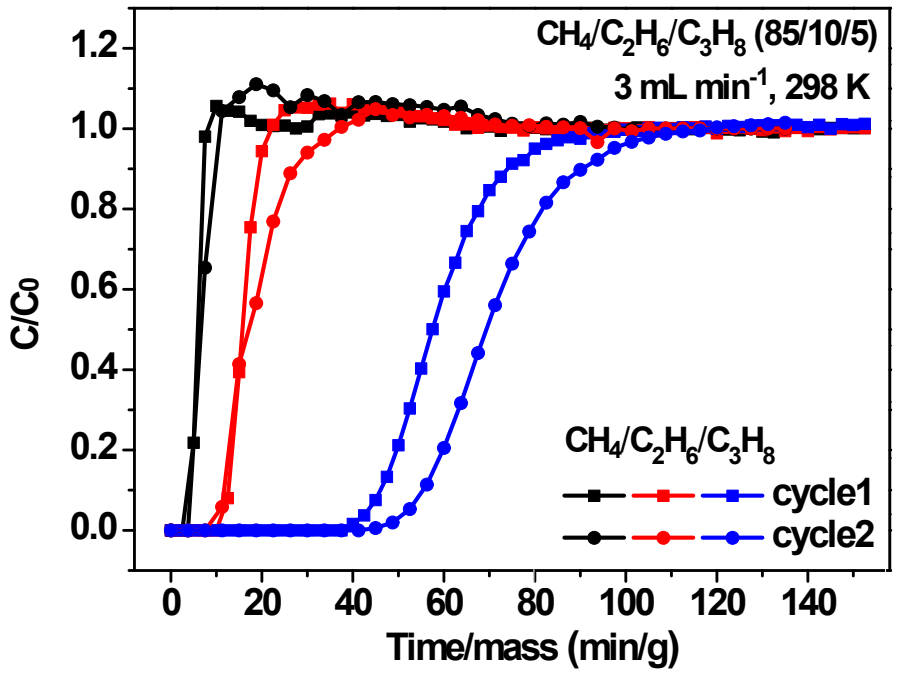

Figure S14. Cycling column breakthrough tests for a $CH_4/C_2H_6/C_3H_8$ (85:10:5, v/v/v) mixture with activated LIFM-233.

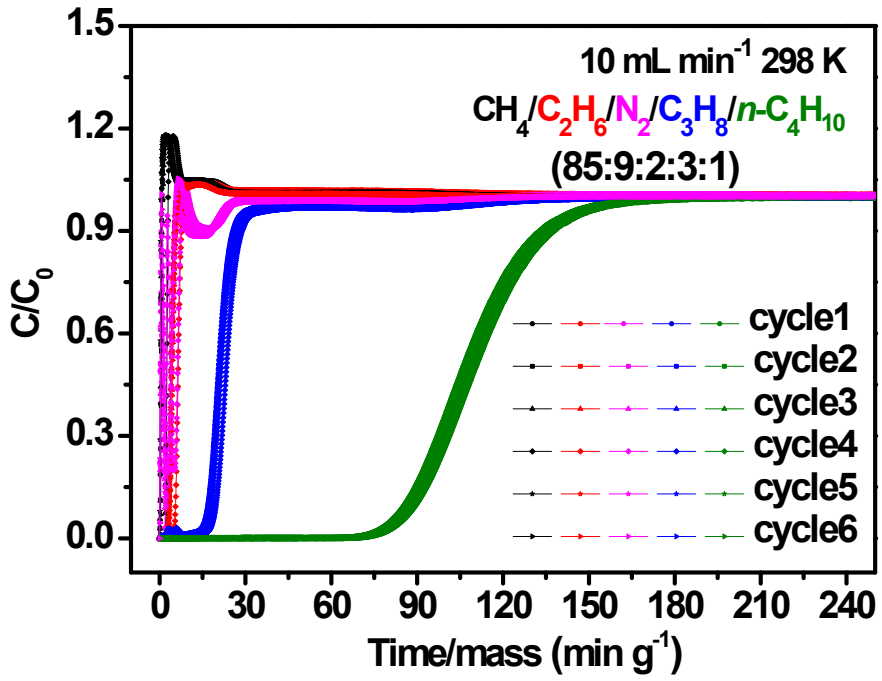

Figure S15. Cycling column breakthrough tests for a $CH_4/C_2H_6/N_2/C_3H_8/n\text{-}C_4H_{10}$ (85:9:2:3:1, v/v/v/v/v) mixture with activated LIFM-233.

S8. Theoretical Calculations

Adsorption site simulations by grand canonical Monte Carlo simulations: The grand canonical Monte Carlo (GCMC) simulations were performed with the Sorption module of Materials Studio.[7] The unit cell of LIFM-233 was used for calculations. After transformed to *P1* space group, hydrogen atoms were added to the Zr cluster for charge balance and the coordinates of all Zr atoms were fixed. Then this initial structure was first optimized using Forcite module with universal force filed (UFF). The convergence tolerances of energy, force and displacement were 2.0×10^{-5} kcal mol^{-1}, 1×10^{-3} kcal mol^{-1} Å^{-1}, and 1×10^{-5} Å, respectively. $CH_4/C_2H_6/C_3H_8/n\text{-}C_4H_{10}$ molecules were directly optimized with Dmol^3. The partial charge of $CH_4/C_2H_6/C_3H_8/n\text{-}C_4H_{10}$ were calculated using the ESP method. The previously described optimized LIFM-233 primitive cell and $CH_4/C_2H_6/C_3H_8/n\text{-}C_4H_{10}$ was used. Atoms in LIFM-233 were fixed during GCMC simulations. The density distributions of the gases in the MOF were

calculated using the fixed pressure task mode of Sorption module under 298 K and 100 kPa (fugacity). The equilibration steps, production steps and temperature were 1×10^6, 1×10^7, and 298 K, respectively. The Dreiding force field was used and the parameters of Zr were adopted from UFF. The van der Waals interactions with a cutoff 18.5 Å were depicted by the Lennard-Jones potential.

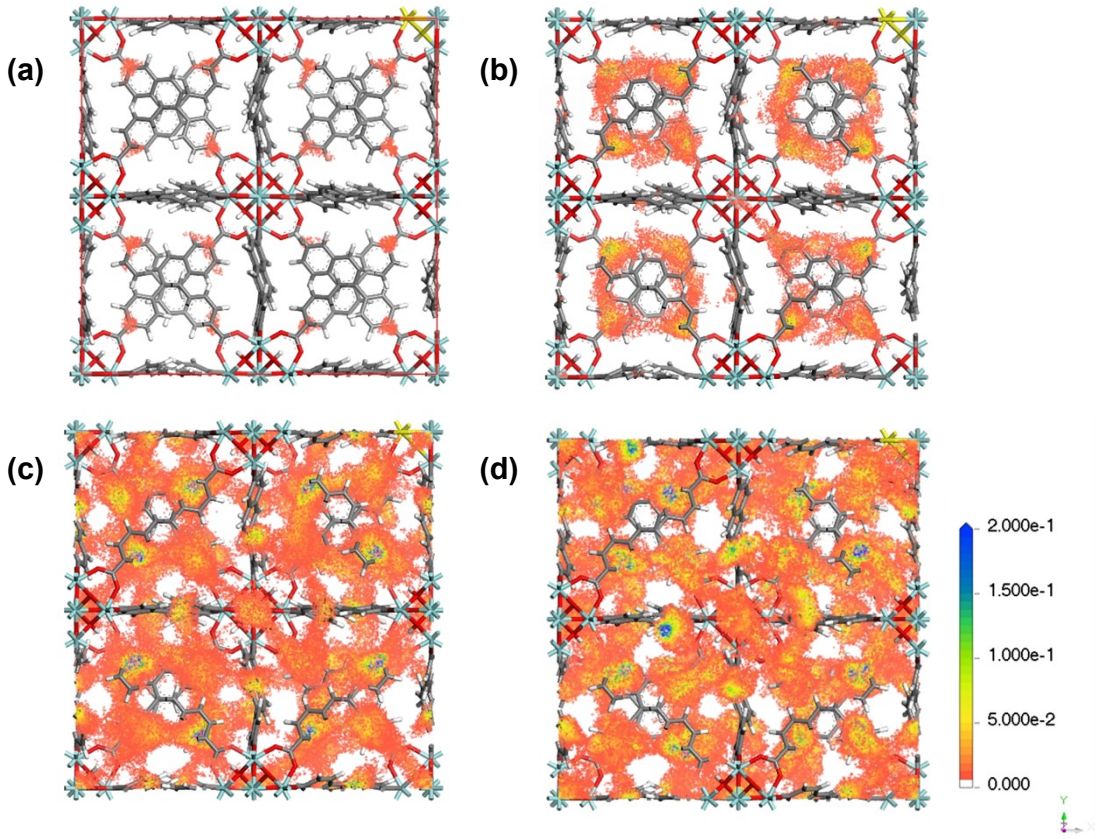

Figure S16. Density distribution of CH_4 (a), C_2H_6 (b), C_3H_8 (c) and *n*-C_4H_{10} (d) in activated LIFM-233 at 298 K and 100 kPa.

S9. Tables

Table S1. Physical parameters of selected gas adsorbates.[8]

Adsorbate	Molecule size /Å^3	Kinetic diameter/Å	Polarizability $\times10^{25}$/cm^3	Dipole moment $\times10^{18}$/esu cm	Quadruple moment $\times10^{26}$/esu cm^2
CH_4	3.76×3.83×3.99	3.758	25.93	0	0
C_2H_6	4.08×4.29×4.72	4.443	44.3-44.7	0	0.65
C_3H_8	4.02×4.79×6.20	4.3-5.118	62.9-63.7	0.084	—
n-C_4H_{10}	4.02×4.61×7.38	4.687	82	0.05	—

Table S2. Crystallographic data of LIFM-233.

MOFs	**LIFM-233**
CCDC	2338023
Empirical formula	C_{108} H_{60} O_{32} Zr_6
Formula weight	2416.88
Temperature[K]	240.00(10)
Radiation Wavelength [Å]	1.54178 (Cu *Kα*)
Crystal system	cubic
Space group	*Fm*-3*m*
a/b/c [Å]	30.0127(4)
α/β/γ[deg]	90
V [Å^3]	27034.3(11)
Z	4
ρ_{calc}[g cm^{-3}]	0.594
μ [mm^{-1}]	2.090
F (000)	4816.0
Crystal size [mm^3]	0.2 × 0.2 × 0.2
2Θ range for data collection [deg]	12.856 to 80.67
Index ranges	-9 ≤ h ≤ 19, -7 ≤ k ≤ 20, -1 ≤ l ≤ 25
Reflections collected	1672
Independent reflections	462 [R_{int} = 0.0209, R_{sigma} = 0.0166]
Data/restraints/parameters	462/320/137
Goodness-of-fit on F^2	1.092
R_1, wR_{2a} [I≥2σ(I)]	0.0426, 0.1080
R_1, wR_{2a} [all data]	0.0490, 0.1147
Largest diff. peak/hole [e. Å^{-3}]	0.23/-0.33

[a] $R_1 = \Sigma||F_o| - |F_c||/|F_o|$; $wR_2 = [\Sigma w(\Sigma F_o^2 - F_c^2)^2/\Sigma w(F_o^2)^2]^{1/2}$.

Table S3. Comparison of selectivities and adsorption capacities for LIFM-233 with previously reported top-performing MOFs.

Adsorbent	Adsorption selectivity		Static adsorption capacity ($cm^3\ g^{-1}$)				T (K)
	C_2H_6/CH_4	C_3H_8/CH_4	CH_4	C_2H_6	C_3H_8	n-C_4H_{10}	
LIFM-233	6.9	98.7	9.0	52.5	229.3	262.8	298
MgMOF-74[9-11]	-	-	24.8	147.8	161.3	-	298
UIO-67(Zr)[10]	8.1[b]	73.7[b]	10.1	67.2	183.7	-	298
UIO-66(Zr)[12, 13]	-	71.5	11.2	51.5	89.6	100.8	298
ECUT-Th-10[13]	-	54.5	9.4	38.5	64.7	60.3	298
Fe_2(dobdc)[14]	32[b]	-	17.2	112.0	127.0	-	313
PAN-p1[15]	16.9	129.3	20.6	84.2	114.5	-	298
0.3Gly@HKUST-1[16]	12.6	173.5	22.8	144.9	174.7	-	298
NKU-FlexMOF-1a[17]	-	-	11.3	69.9	65.7	70.8	298
Ni(TMBDC)$(DABCO)_{0.5}$[18]	29[b]	274[b]	35.8	130.1	124.1		298
UTSA-35a[19]	8	80	9.5	53.7	73.2	-	296
CoMOF-74[11, 20]	26.0	290.0	33.5	168.8	136.1	-	296
RT-MIL-100(Fe)[21]	6	33.3	8.1	49.7	151.9	-	298
MIL-101-Cr[22]	22.5	84.3	11.0	35.6	75.0	-	298
MIL-142A[23]	13.7	1300.0	12.1	85.6	119.2		298
C-PVDC-800[24]	74.9	3387.2	34.5	118.5	115.8		298
CAU-3-NDCA[25]	8.4	879.9	7.7	52.9	177.8		298
BSF-2[26]	53.0	2609.0	5.4	27.3	39.6		298
TIFSIX-Cu-TPA[27]	16.2	68.6	15.2	98.6	110.0		298
Ni(HBTC)(bipy)[28]	27.5	1857.0	20.8	131.0	138.4		298
Co-MOF[29]	26.0[b]	290.0[b]	16.6	58.6	59.4		298
CTGU-15[30]	5.2	170.7	8.9	47.7	271.7		298
JUC-100[31]	10.7	82.3	10.2	92.1	136.0		298
Iso-MOF-4[32]	8.5	80.0	13.4	114.0	240.9		298
InOF-1[33]	17.0	90.0	14.3	92.7	95.2		298

[a] Unless otherwise stated, the data was calculated under the condition of equimolar binary mixtures and 1 bar;

[b] IAST selectivity calculated under the condition of C_2H_6/CH_4 = 10/85 or C_3H_8/CH_4 = 5/85 and 1 bar.

Table S4. Comparison of **LIFM-233** with various other adsorbents for C_1-C_4 hydrocarbon separation in terms of the CH_4 productivity, $C_2H_6/C_3H_8/n\text{-}C_4H_{10}$ capture capacity, and recovered $C_3H_8/n\text{-}C_4H_{10}$ purity based on a ternary $CH_4/C_3H_8/n\text{-}C_4H_{10}$ or quinary $CH_4/C_2H_6/N_2/C_3H_8/n\text{-}C_4H_{10}$ transient adsorption-desorption breakthrough experiment.

Adsorbent	Flow rate of gas mixture	CH_4 productivity (mmol g^{-1})	Dynamic adsorption uptake (mmol g^{-1})			Recovery purity	
			C_2H_6	C_3H_8	$n\text{-}C_4H_{10}$	C_3H_8	$n\text{-}C_4H_{10}$
LIFM-233[b]	10	1.17	0.12	0.33	0.48	92.7	94.0
LIFM-233	3	1.23	0.25	0.50	-	91.6	-
C-PVDC-800[24]	2	15.72	-	3.02	-	-	-
CAU-3-NDCA[25]	10	-	0.25	0.446	-	-	-
BSF-2[26]	4	-	-	0.759	-	-	-
TIFSIX-Cu-	4	5	-		-	-	-
Ni(HBTC)(bipy)[28]	10	-	1.21	3.0	-	-	-
Co-MOF[29]	2	1.59	0.78	0.50	-	-	-
MIL-101-Cr[22]	2	-	0.25	0.60	-	-	-
MIL-101-Fe[22]	3	-	0.49	0.29	-	-	-
CTGU-15[30]	2	-	-	0.38	-	-	-

[a] Unless otherwise stated, the data was calculated under the condition of $C_3H_8/C_2H_6/CH_4$ (5:10:85, v/v/v) and 1 bar;

[b] The data was calculated under the condition of $CH_4/C_2H_6/N_2/C_3H_8/n\text{-}C_4H_{10}$ (85:9:2:3:1, v/v/v/v/v) and 1 bar.

S10. References

1. V. Sharma, D. De, S. Pal, P. Saha and P. K. Bharadwaj, *Inorg. Chem.*, **2017**, *56*, 8847-8855.
2. G. Sheldrick, *Acta Crystall. A*, **2008**, *64*, 112-122.
3. A. Spek, *Acta Crystall. C*, **2015**, *71*, 9-18.
4. J. L. C. Rowsell, O. M. Yaghi, *J. Am. Chem. Soc*., **2006**, *128*, 1304-1315.
5. A. L. Myers, J. M. Prausnitz, *AIChE J.*, **1965**, *11*, 121-127.
6. Y. S. Bae, K. L. Mulfort, H. Frost, P. Ryan, S. Punnathanam, L. J. Broadbelt, J. T. Hupp, R. Q. Snurr, *Langmuir*, **2008**, *24*, 8592-8598.
7. P.-Q. Liao, N.-Y. Huang, W.-X. Zhang, J.-P. Zhang, X.-M. Chen, *Science,* **2017**, *356*, 1193-1196..
8. J.-R. Li, R. J. Kuppler and H.-C. Zhou, *Chem. Soc. Rev.*, **2009**, *38*, 1477-1504.
9. Z. Bao, S. Alnemrat, L. Yu, I. Vasiliev, Q. Ren, X. Lu and S. Deng, *Langmuir*, **2011**, *27*, 13554-13562.
10. Y. Zhang, H. Xiao, X. Zhou, X. Wang and Z. Li, *Ind. Eng. Chem. Res.*, **2017**, *56*, 8689-8696.
11. Y. He, R. Krishna and B. Chen, *Energ. Environ. Sci.*, **2012**, *5*, 9107-9120.
12. F. Ahmadijokani, S. Ahmadipouya, H. Molavi, M. Rezakazemi, T. M. Aminabhavi and M. Arjmand, *J. Environ. Manage.*, **2020**, *274*, 111155.
13. L. Wang, W. Zhang, J. Ding, L. Gong, R. Krishna, Y. Ran, L. Chen and F. Luo, *Nano Res.*, **2023**, *16*, 3287-3293.
14. E. Bloch, W. Queen, R. Krishna, J. Zadrozny, C. Brown, J. R Long,. *Science* **2012**, *335*, 1606−1610.
15. G. Li and Z. Wang, *ACS Appl.Mater. Interfaces*, **2020**, *12*, 24488-24497.
16. Y. Wu, Y. Sun, J. Xiao, X. Wang and Z. Li, *ACS Sustainable Chem. Eng.*, **2019**, *7*, 1557-1563.
17. M.-H. Yu, B. Space, D. Franz, W. Zhou, C. He, L. Li, R. Krishna, Z. Chang, W. Li, T.-L. Hu and X.-H. Bu, *J. Am. Chem. Soc.*, **2019**, *141*, 17703-17712.
18. Y. Wu, Z. Liu, J. Peng, X. Wang, X. Zhou and Z. Li, *ACS Appl.Mater. Interfaces*, **2020**, *12*, 51499-51505.
19. Y. He, Z. Zhang, S. Xiang, F. R. Fronczek, R. Krishna and B. Chen, *Chem. Commun.*, **2012**, *48*, 6493-6495.
20. P. D. C. Dietzel, Y. Morita, R. Blom and H. Fjellvåg, *Angew. Chem. Int. Ed.*, **2005**, *44*, 6354-6358.
21. B. Yuan, X. Wang, X. Zhou, J. Xiao and Z. Li, *Chem. Eng. J.*, **2019**, *355*, 679-686.
22. L.-Z. Qin, X.-H. Xiong, S.-H. Wang, L. Zhang, L.-L. Meng, L. Yan, Y.-N. Fan, T.-A. Yan, D.-H. Liu, Z.-W. Wei and C.-Y. Su, *ACS Appl. Mater. Interfaces*, **2022**, *14*, 45444-45450.
23. Y. Yuan, H. Wu, Y. Xu, D. Lv, S. Tu, Y. Wu, Z. Li and Q. Xia, *Chem. Eng. J.*, **2020**, *395*, 125057.

24. F. Chen, K. Guo, X. Huang, Z. Zhang, Q. Yang, Y. Yang, Q. Ren and Z. Bao, *Sci. China. Mater.*, **2023**, *66*, 319-326.
25. M. Chang, C. Yang, M. Tong, J. Yang, T. Ma, S. Jiao, Q. Ma, Y. Wang, D. Liu and J. Zheng, *Ind. Eng. Chem. Res.*, **2024**, *63*, 2851-2860.
26. Y. Zhang, L. Yang, L. Wang, X. Cui and H. Xing, *J. Mater. Chem. A*, **2019**, *7*, 27560-27566.
27. Y. Chen, Y. Jiang, J. Li, X. Hong, H. Ni, L. Wang, N. Ma, M. Tong, R. Krishna and Y. Zhang, *AIChE J.*, **2024**, *70*, 18320.
28. P. Guo, M. Chang, T. Yan, Y. Li and D. Liu, *Chin. J. Chem. Eng.*, **2022**, *42*, 10-16.
29. L. Lan, N. Lu, J.-C. Yin, Q. Gao, F. Lang, Y.-H. Zhang, H.-X. Nie, N. Li and X.-H. Bu, *Chem. Eng. J.*, **2023**, *476*, 146750.
30 D. Lv, Z. Liu, F. Xu, H. Wu, W. Yuan, J. Yan, H. Xi, X. Chen and Q. Xia, *Sep. Purif.*, **2021**, *266*, 118198.
31. J. T. Jia, L. Wang, F. X. Sun, X. F. Jing, Z. Bian, L. X. Gao, R. Krishna and G. S. Zhu, *Chem. Eur. J.,* **2014***, 20*, 9073-9080.
32. W.D. Fan, X. Wang, X.R. Zhang, X.P. Liu, Y.T. Wang, Z.X. Kang, F.N. Dai, B. Xu, R.M. Wang, D.F. Sun, *ACS Cent. Sci*., **2019**, *5*, 1261-1268.
33. Y.W. Chen, Z.W. Qiao, D.F. Lv, H.X. Wu, R.F. Shi, Q.B. Xia, H.H. Wang, J. Zhou, Z. Li, *Ind. Eng. Chem. Res.*, **2017**, *56*, 4488-4495.